ACS OMEGA

In Situ Surface Engineering of Mesoporous Silica Generates Interfacial Activity and Catalytic Acceleration Effect

Fengwei Zhang,[*,†] Juan Li,[†] Xincheng Li,[‡] Mengqi Yang,[‡] Hengquan Yang,[*,†,‡] and Xian-Ming Zhang[*,†]

[†]Institute of Crystalline Materials and [‡]School of Chemistry and Chemical Engineering, Shanxi University, Taiyuan 030006, P. R. China

⑤ *Supporting Information*

ABSTRACT: Mesoporous structured catalysts featuring interfacial activity are the most promising candidates for biphasic interface catalysis because their nanopores can concurrently accommodate catalytic active components and provide countless permeable channels for mass transfer between the interior and the exterior of Pickering droplets. However, to date, a convenient and effective strategy for the preparation of an anchor site-containing interfacial active mesoporous catalyst is still lacking. In the present work, we report a novel and efficient interfacial active mesoporous silica (MS) catalyst, which is prepared by a facile cocondensation of two types of organosilanes and subsequent anchoring of Pd NPs onto its

surface through the confinement and coordination interactions. The as-prepared catalyst is then applied as emulsifier to stabilize the water-in-oil (W/O) Pickering emulsion and investigated as an interfacial catalyst for the hydrogenation of nitroarenes. An obviously enhanced rate toward the nitrobenzene hydrogenation is observed for the 0.8 mol% Pd/PAP-functionalized mesoporous silica-20 catalyst in the emulsion system (both conversion and selectivity are >99% within 30 min) in comparison to a single aqueous solution. Moreover, the emulsion catalytic system can be easily recycled six times without the separation of the catalyst from the water phase during the recycling process. This finding demonstrates that the incorporation of phenylaminopropyl trimethoxysilane amphiphilic groups during the hydrolysis of tetramethyl orthosilicate not only endows MS with interfacial activity but also improves the catalytic activity and stability.
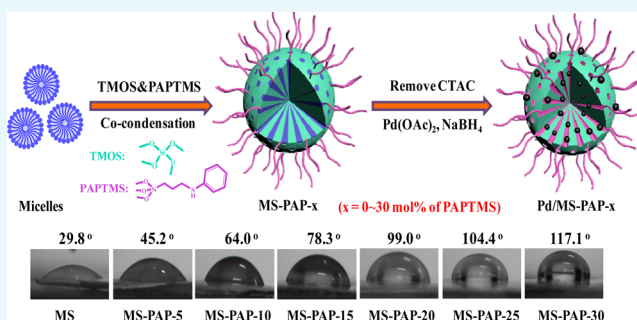
1. INTRODUCTION

One kind of liquid dispersed in another kind of liquid in the form of droplets is called an emulsion; emulsions are seen in many fields in our daily life.[1−3] The associated emulsifiers are commonly used to prohibit the coalescence between the droplets and to obtain a stable microemulsion system without the macroscopic phase separation. Apart from the surfactant molecules, emulsifiers can also be micrometer- or nanometer-scaled colloidal particles that locate at the liquid−liquid two-phase interface and generate a protective film between the dispersed and continuous phases.[4−7] These colloidal particle-stabilized emulsions are named "Pickering emulsions" by Pickering in 1907.[8] After that, numerous efforts have been made on developing particulate emulsifiers for the preparation of Pickering emulsions. The advantages distinguishing the Pickering emulsion from the conventional emulsions stabilized by surfactants are its ultrahigh stability, low toxicity, simple separation, and well-adjustable droplet size.[9−13] Considering these characteristics and advantages, the Pickering emulsion has attracted increasing attention in various fields such as cosmetics, coatings, foods, crude oil recovery, wastewater treatment, and biomedical applications.[14−19] Beyond all this, the heterogeneous catalysts based on Pickering emulsion have

also received widespread attention in hydrogenation, oxidation, biomass conversion, esterification reactions, and so forth.[20−23]

Over the past decade, it has been demonstrated that the Pickering emulsion plays an accelerating effect by virtue of solubilization of the hydrophobic substrates in an aqueous solution followed by their activation by the surface-assembled catalyst in the interior or exterior of the droplets. Furthermore, the product is dissolved in the organic phase, and the catalyst is located in the aqueous phase after centrifugation, thus simplifying the product isolation and catalyst recycling. In general, the frequently used approach for the synthesis of amphiphilic nanocomposites adopts harsh conditions or tedious postgrafting methods. For example, Resasco and co-workers prepared a variety of amphiphilic hybrid nanoparticles (NPs) by fusing hydrophobic carbon nanotubes to hydrophilic inorganic NPs (SiO₂, MgO, NaX, and Al₂O₃) and then supported precious-metal NPs for biofuel upgrade, glucose cascade, and F−T synthesis.[24−27] Qi et al. have prepared an amphiphilic Janus particle through multistep region-selective modification toward the oil/water two-phase enzyme catal-
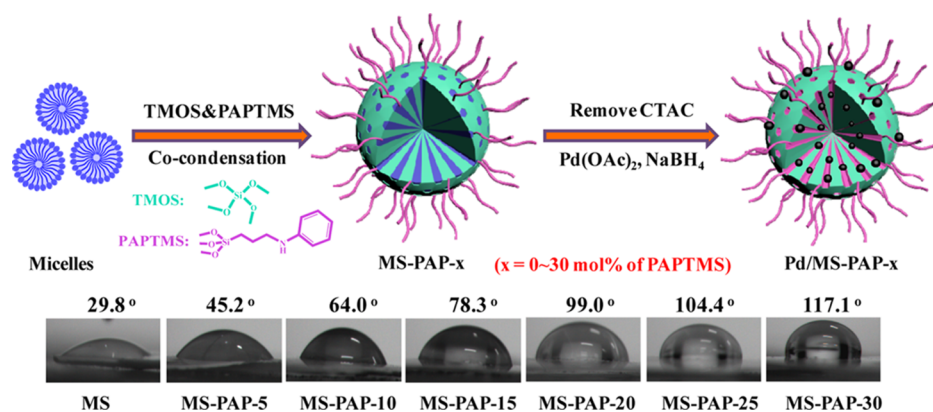
Figure 1. Schematic description of the fabrication of Pd/MS-PAP-*x* (*x* denotes the molar ratio of PAPTMS to TMOS) and the corresponding contact angle (CA) test results.

ysis.[28] Recently, our groups have successfully prepared an interfacial active mesoporous silica (MS) catalyst through functionalization with octyl groups, which shows dramatically enhanced catalytic activity in the hydrogenation of aqueous olefins. However, the preparation procedure of the MS catalyst requires a step-by-step hydrolysis pathway, and the mesoporous internal/external surfaces lack amino or other functional groups for the stabilization of precious-metal NPs.[29] Therefore, it is highly desirable to develop a straightforward and mild reaction strategy to fabricate an interfacial active MS catalyst whose internal/external surfaces have abundant amino groups anchoring sites.

Inspired by these approaches, herein we describe the synthesis of a novel and efficient interfacial active mesoporous catalyst, where interfacial active MS is generated in situ by a simple cocondensation of tetramethyl orthosilicate (TMOS) and phenylaminopropyl trimethoxysilane (PAPTMS) organosilanes, and subsequent anchoring of Pd NPs onto its surface through the confinement and coordination interactions. It is particularly worth mentioning that PAPTMS can act as (i) a surface modifier for adjusting the wettability of MS and (ii) a stabilizing and supporting agent for the uniform and high dispersion of Pd NPs. In this study, a series of interfacial active mesoporous catalysts are successfully prepared via simply altering the PAPTMS mole fraction with respect to the TMOS silica source precursor. Optical microscopy analysis indicates that the as-synthesized Pd/PAP-functionalized mesoporous silica (MS-PAP)-20 catalyst can be used as an emulsifier to create a stable water-in-oil (W/O) Pickering emulsion in ethyl acetate/H_2O two-phase systems, and the average diameter of the droplet is around 175 ± 12 μm. Furthermore, the catalytic results demonstrate that the catalyst is highly efficient for the hydrogenation of various nitroarenes and its original catalytic properties can be retained even after recycling six times.

2. EXPERIMENTAL SECTION

2.1. Materials. Cetyltrimethylammonium chloride (CTAC, 99%) was purchased from Nanjing Robiot Co., Ltd. Palladium-(II) acetate [Pd(OAc)$_2$, ≥97%], TMOS (98%), and sodium hydroxide (NaOH) were purchased from Sinopharm Chemical Reagent Co., Ltd. PAPTMS and sodium borohydride (NaBH$_4$, 98%) were obtained from Aladdin Chemical Reagent Co., Ltd. All other chemicals were of analytical grade and were used without any further purification.

2.2. Preparation of MS-PAP. A representative MS-PAP-20 sphere was synthesized according to our previous publication, with some modifications.[30] Typically, 3.52 g of CTAC and 2.5 mL of NaOH (1.0 mol/L) were added to a mixture of 500 mL of methanol and 400 mL of deionized water in a round-bottom flask. After stirring at room temperature for 30 min, 2.64 g of TMOS and 0.84 g of PAPTMS were added together to the solution dropwise under stirring. The above solution was continuously stirred for 10 h and then left to settle overnight. The generated white product was collected by vacuum filtration, thoroughly washed with deionized water and ethanol, and dried at 80 °C for 18 h. To remove the pore-generating template (CTAC), the as-synthesized sample was transferred into an ethanol solution containing ammonium nitrate (0.5 g/ 150 mL) and stirred for 1.0 h under reflux, and the extraction step was repeated two times to ensure complete removal of CTAC. The template-removed MS-PAP-20 sphere was washed with deionized water and ethanol three times and dried at 80 °C overnight under vacuum. MS spheres with different surface wettabilities were obtained by adjusting the loading amount of PAPTMS during the cocondensation process (the molar quantity of PAPTMS was changed from 0 to 30 mol % with respect to TMOS), and the samples were denoted as MS, MS-PAP-5, MS-PAP-10, MS-PAP-15, MS-PAP-20, MS-PAP-25, and MS-PAP-30.

2.3. Loading of Pd NPs on MS-PAP. To a stirred suspension of MS-PAP-20 (1.0 g) in 30 mL of toluene was added 65 mg of Pd(OAc)$_2$. After stirring for 4 h [the amount of Pd(OAc)$_2$ adsorbed onto the solid materials was calculated using UV–vis spectra], 20 mL of NaBH$_4$ (120 mg) was slowly added and stirred for another 4 h. The suspension was centrifuged and washed several times with deionized water and ethanol, resulting in Pd/MS-PAP-20 (the loading amount of Pd was 3.02 wt %).

2.4. Pd/MS-PAP Catalyst for the Hydrogenation of Nitroarenes. The liquid-phase hydrogenation of nitroarenes was carried out in a 10 mL glass vessel. In a typical procedure, 30 mg of Pd/MS-PAP (0.8 mol %), 1.0 mmol of nitroarenes, 1.0 mL of toluene or ethyl acetate, and 1.0 mL of deionized water were placed in the vessel. After the replacement of air with H$_2$ for three times, the mixture was then stirred at 25 °C for a certain period of time in an atmospheric hydrogen balloon. The reaction process was monitored using an Agilent 7890A gas chromatographic analyzer.

2.5. Characterization. Transmission electron microscopy (TEM) analysis was carried out using a FEI Tecnai G2 F20S-
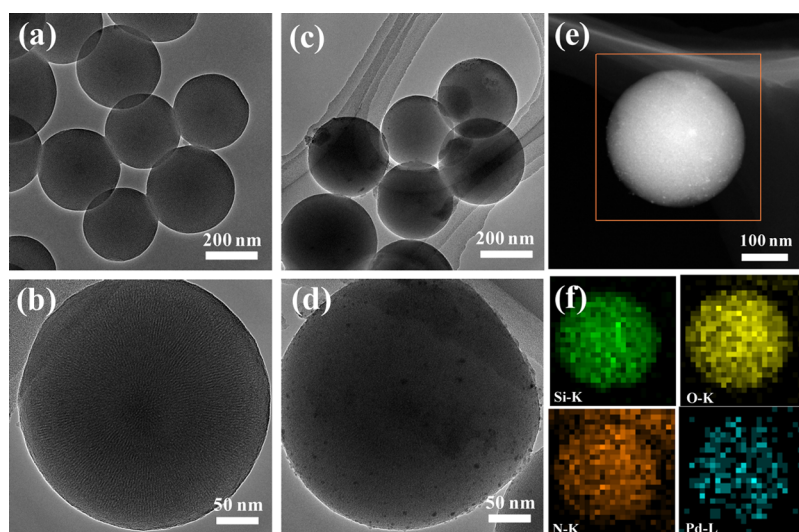
Figure 2. TEM and magnified TEM images of (a,b) MS-PAP-20, (c,d) Pd/MS-PAP-20, and (e,f) high-angle annular dark-field scanning TEM (HAADF-STEM) and elemental mapping images of the Pd/MS-PAP-20 catalyst.
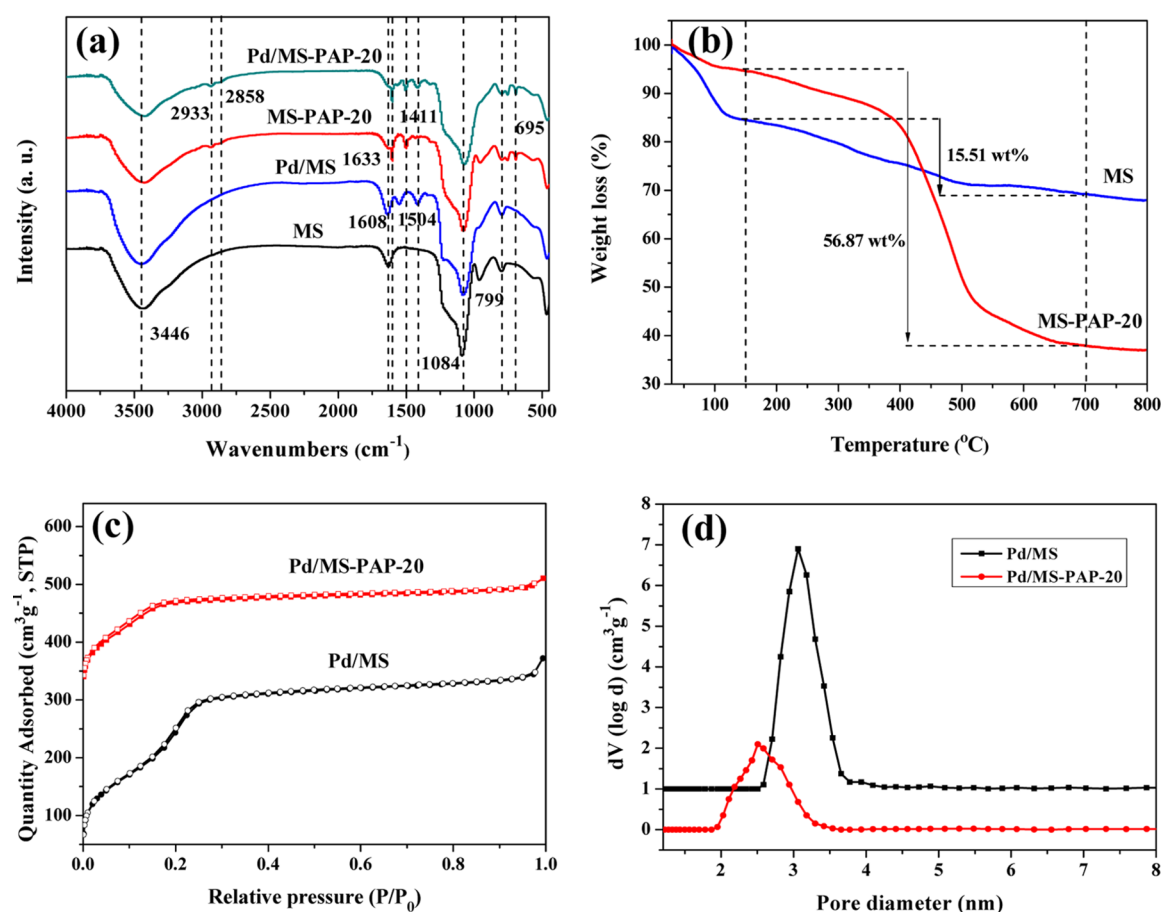

Figure 3. (a) FTIR spectra, (b) TGA curves, (c) N_2 adsorption−desorption isotherms, and (d) the corresponding pore size distribution of the as-synthesized MS samples.

Twin microscope at a 200 kV accelerating voltage. For sample preparation, the powders were dispersed in an ethanol solution through sonication, and then one drop of the suspension was dropped onto a microgrid. Fourier transform infrared (FTIR) spectra were obtained using a Nicolet iS5 spectrophotometer (frequency range from 4000 to 500 cm^{-1}) with a KBr pellet. Thermogravimetric analysis (TGA) was performed on a

Setaram Evolution 16/18 apparatus. The samples were heated in an alumina pan from 30 to 800 °C at a heating rate of 10 °C/min under a high-purity nitrogen atmosphere. The N_2 adsorption−desorption isotherms were obtained on a Quantachrome autosorb iQ$_2$ analyzer. Before measurement, the samples were first degassed under vacuum at 393 K for 6 h at a heating rate of 5 °C/min. The specific surface areas of the
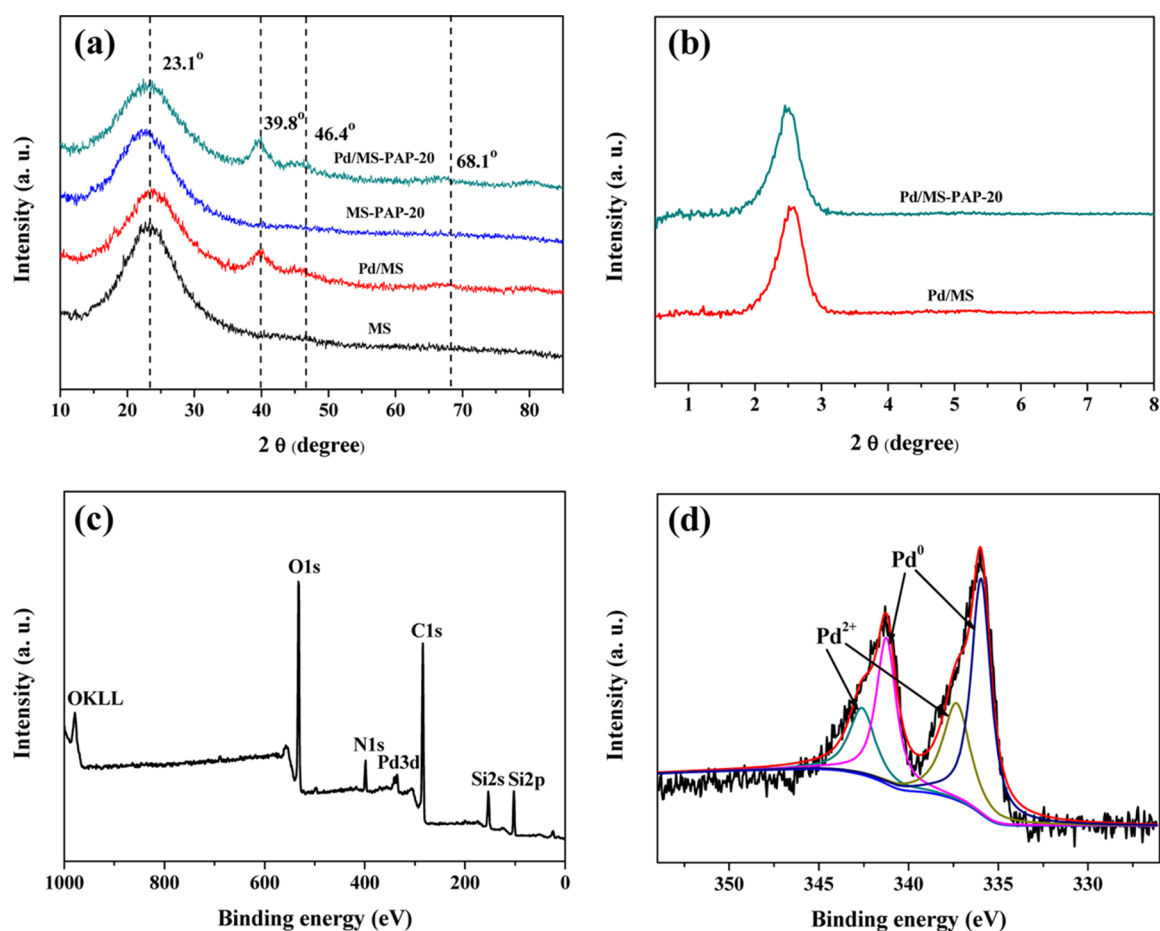
Figure 4. (a,b) Wide-angle and small-angle XRD patterns and (c,d) XPS spectra of the elemental survey scan and the Pd 3d scan.
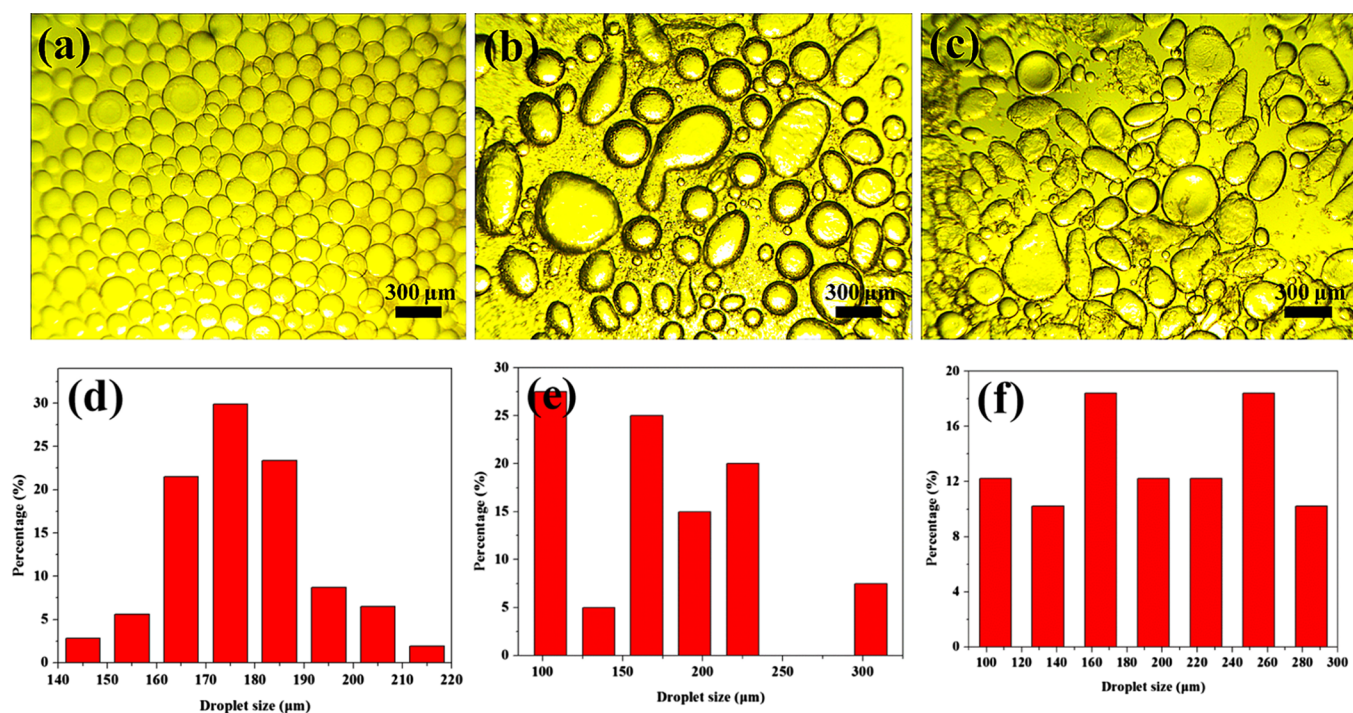

Figure 5. Optical microscopy images and droplet size distribution of the Pd/MS-PAP-20-stabilized Pickering emulsion in different biphasic systems: (a,d) ethyl acetate/H_2O, (b,e) toluene/H_2O, and (c,f) cyclohexane/H_2O.
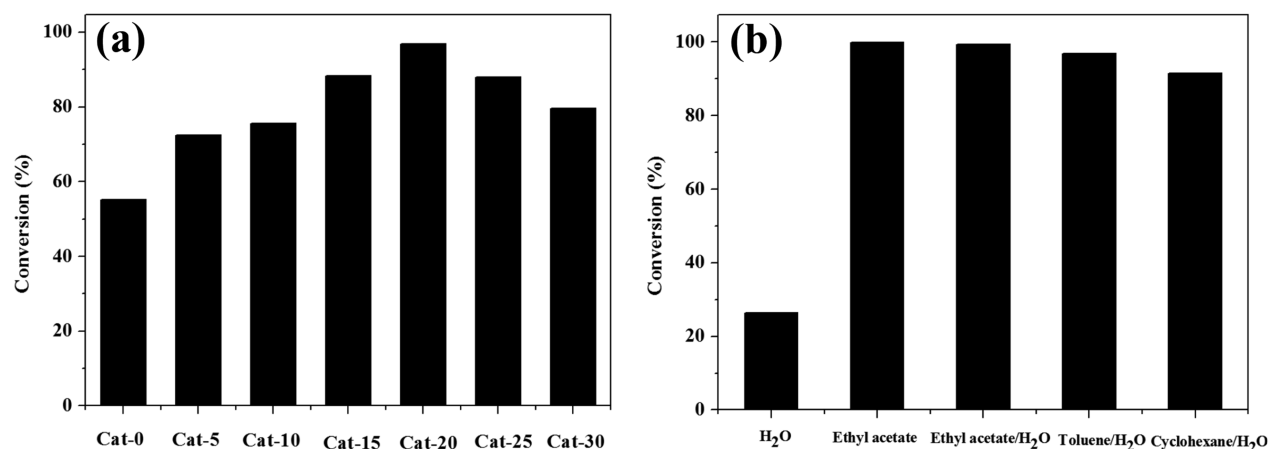
Figure 6. (a) Influence of the loading amount of PAP organosilane on the catalytic activity (the abbreviation Cat-0 to Cat-30 stands for Pd/MS to Pd/MS-PAP-30 catalysts, respectively) and (b) influence of solvent type on the catalytic performance of the Pd/MS-PAP-20 catalyst.

samples were calculated using the Brunauer–Emmet–Teller (BET) method; pore size distribution and pore volume were calculated using the Barrett–Joyner–Halenda (BJH) model. X-ray diffraction (XRD) measurements were recorded on a Rigaku Ultima IV diffractometer using Cu-Kα radiation as the X-ray source in the 2θ range of $10°–80°$. The X-ray photoelectron spectra (XPS) were recorded on the PHI-5702 instrument, and the C_{1s} line at 284.5 eV was used as the binding-energy reference.

3. RESULTS AND DISCUSSION

3.1. Material Preparation and Characterization. Preparation of MS catalyst with interfacial activity involves a simple two-step route via the combination of cocondensation of different organosilanes and the adsorption–reduction metal precursor strategy. Specifically, TMOS and PAPTMS were chosen as the support framework and surface-modifying agent, respectively, which were cohydrolysed in an alkaline methanol–water solution in the presence of CTAC (the pore-forming agent). Subsequently, the Pd NPs were embedded in the mesoporous pore under the confinement and coordination interactions after the removal of the CTAC template. The resulting samples were denoted as Pd/MS-PAP-x (x is continuously changed from 0 to 30 mol %), where x stands for the molar fraction of PAPTMS with respect to TMOS. The surface wettability of the MS-PAP-x support displayed the water CA as it was gradually increased from 29.8° to 45.2°, 64.0°, 78.3°, 99.0°, 104.4°, and 117.1°, indicating the continuous increase in the hydrophobic PAPTMS unit and decrease in the hydrophilic TMOS silica source (Figure 1).
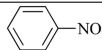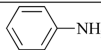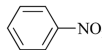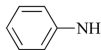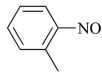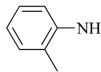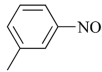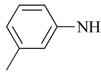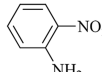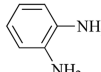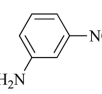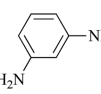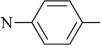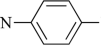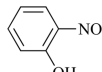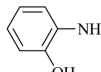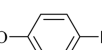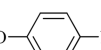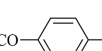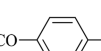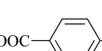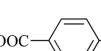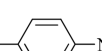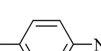
The morphology and the microstructure of MS-PAP-20 and Pd/MS-PAP-20 samples were investigated using TEM. As can be seen from Figure 2a,b, the MS-PAP-20 microsphere possesses excellent dispersibility and the average diameter is approximately 305 nm. Moreover, the surface of an individual microsphere contains a plentiful of about 2.7 nm (as shown in Figure S1) perpendicularly oriented channels, which is advantageous for the transference of metal precursors and substrate molecules. In contrast, the shape and size of the Pd/MS-PAP-20 catalyst did not show obvious change even after immobilization of the tiny Pd NPs. The magnified TEM image of the Pd/MS-PAP-20 catalyst incontrovertibly proves that a certain amount of Pd NPs with 2.0 nm are well-embedded in the mesoporous channels via confinement effect and that others

are probably immobilized on the MS-PAP-20 support surface (Figure S2). However, the Pd NPs are mainly centered at 2.5 ± 0.5 nm for the Pd/MS catalyst. A representative HAADF-STEM image directly demonstrates a homogeneous distribution of Si, O, N, and Pd elements on the Pd/MS-PAP-20 catalyst surface, and the Pd atoms are completely surrounded by a large number of N atoms.

The successful incorporation of organic units is further characterized by using a FTIR spectrometer. Figure 3a exhibits the spectra of MS, Pd/MS, MS-PAP-20, and Pd/MS-PAP-20. The broad absorption peaks at 3446 and 1084 cm^{-1} can be attributed to the surface-adsorbed water, −OH, and Si−O−Si stretching vibrations.[31,32] For MS-PAP-20 and Pd/MS-PAP-20 samples, the peaks at around 2933, 2858, and 1411 are ascribed to the C−H asymmetric, C−H symmetric, and C−H bending vibrations of −CH$_2$ groups, respectively, whereas the peak at 695 cm^{-1} is attributed to the C−H out-of-plane bending vibration of the benzene ring in the PAPTMS units.[33] The band at 1608 cm^{-1} can be assigned to the N−H deformation vibration, confirming the presence of amine groups.[34,35] The loading amount and the thermal stability of the phenyl-aminopropyl (PAP) organic component are evaluated using TGA under a nitrogen atmosphere. As shown in Figure 3b, the TGA curve of MS presents 15.4 wt % weight loss at around 150 °C because of the evaporation of physiadsorbed water. Comparatively, the weight loss of MS-PAP-20 is dramatically decreased to 5.2 wt % below 150 °C, suggesting a greater hydrophobic property. The difference in weight loss between MS and MS-PAP-20 in the range of 150−700 °C indicates the loading amount of PAP component up to 41.4 wt %. The result demonstrates that more than 95% of the 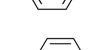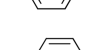initial PAPTMS organosilane is incorporated into the MS microspheres. The textural properties of these two catalysts are evaluated using N$_2$ adsorption−desorption analysis (Figure 3c). The isotherms of Pd/MS and Pd/MS-PAP-20 catalysts are of type IV in the IUPAC classification, which is characteristic of mesoporous materials. Their specific surface area and pore volume are 715 m^2·g^{-1}, 0.599 cm^3·g^{-1} and 244 m^2·g^{-1}, 0.264 cm^3·g^{-1}, respectively. The pore size distribution curves display the pore size of MS contracted from 3.1 to 2.5 nm.

The XRD patterns of Pd/MS and Pd/MS-PAP-20 catalysts show three more diffraction peaks at around 39.8°, 46.4°, and 68.1° except for the amorphous silica peak at 23.1°, which are characteristics of the face-centered-cubic metallic Pd. Figure 4b

Table 1. Hydrogenation of Various Substrates Using Pd/MS-PAP-20 as the Catalyst[a]

Entry	Substrate	Product	t (min)	Conv. (%)[b]	Sel. (%)[b]
1	C6H5–NO2	C6H5–NH2	30	>99	>99
2[c]	C6H5–NO2	C6H5–NH2	60	63.2	>99
3	2-methylnitrobenzene	2-methylaniline	45	>99	>99
4	3-methylnitrobenzene	3-methylaniline	45	>99	>99
5	2-nitroaniline (NO2, NH2)	benzene-1,2-diamine (NH2, NH2)	60	>99	>99
6	3-nitroaniline (NO2, H2N)	benzene-1,3-diamine (NH2, H2N)	30	>99	>99
7	H2N–C6H4–NO2	H2N–C6H4–NH2	60	>99	>99
8	2-nitrophenol (NO2, OH)	2-aminophenol (NH2, OH)	30	>99	>99
9	HO–C6H4–NO2	HO–C6H4–NH2	30	>99	>99
10	H3CO–C6H4–NO2	H3CO–C6H4–NH2	30	>99	>99
11	H3COOC–C6H4–NO2	H3COOC–C6H4–NH2	60	>99	>99
12	F–C6H4–NO2	F–C6H4–NH2	30	>99	>99
13	Cl–C6H4–NO2	Cl–C6H4–NH2	45	>99	86.1
14	Br–C6H4–NO2	Br–C6H4–NH2	45	94.0	>99
15	OHC–C6H4–NO2	OHC–C6H4–NH2	45	>99	98.8

[a]Reaction conditions: 30 mg of catalyst (0.8 mol %), 1 mmol of substrate, 1.0 mL of ethyl acetate, 1.0 mL of water, 25 °C, and atmospheric H_2 balloon. [b]Conversion and selectivity are determined using an Agilent 7890A gas chromatograph. [c]Hydrogenation with 20 mg of 5 wt % Pd/C catalyst (0.8 mol %).

displays the small-angle XRD patterns of the as-prepared samples. It is clearly seen that the two materials exhibit a broad reflection peak in the range of $2\theta = 2°–3°$, indicating the existence of a mesoporous structure, which is well-consistent with the results of the TEM and N_2 adsorption–desorption analyses. The XPS results show that Si, O, C, N, and Pd elements are detected on the surface of the Pd/MS-PAP-20 catalyst. The Pd 3d spectrum of the catalyst is shown in Figure 4d. The shoulder peaks centered at around 336.0 and 341.2 eV are ascribed to Pd^0 $3d_{3/2}$ and Pd^0 $3d_{5/2}$, whereas the peaks at 337.4 and 342.6 eV are attributed to Pd^{2+} $3d_{3/2}$ and Pd^{2+} $3d_{5/2}$.[36] The percentage of Pd^0 and Pd^{2+} species is calculated

from the relative areas of these four peaks, which show that approximately 63.2% of Pd^{2+} ions are reduced into Pd NPs through chemical reduction with $NaBH_4$. Moreover, it should be noted that a certain amount of metal Pd NPs may be encapsulated into the MS channels by the confinement effect.

To gain insights into the morphology of the droplets and the size of the Pd/MS-PAP-20-stabilized Pickering emulsion in various biphasic systems, optical microscopy was used to observe the assembly behavior of the interfacial active catalyst. From Figure 5a,d, it can be seen that the Pd/MS-PAP-20 catalyst is well-adsorbed on the ethyl acetate/H_2O two-phase interfaces, forming finely dispersed spherical emulsion droplets,
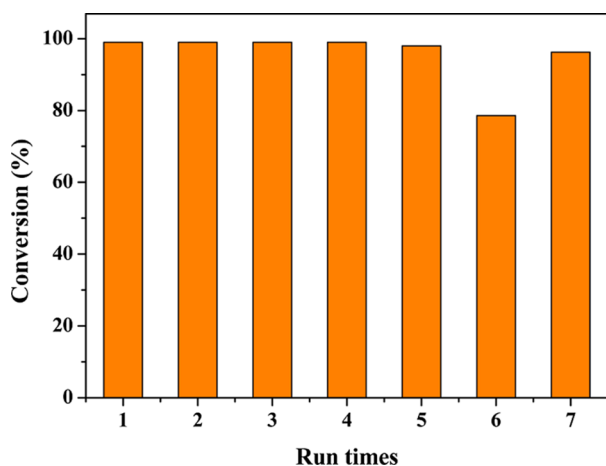
Figure 7. Recyclability of the Pd/MS-PAP-20 catalyst in the hydrogenation of nitrobenzene.

and the droplet size is mainly distributed in the range of 163–188 μm. In comparison, the droplets present obvious irregular shapes in toluene/H$_2$O and cyclohexane/H$_2$O biphasic systems, and the droplet size has a large range fluctuation (Figure 5b,c). In addition, a considerable amount of catalyst particles are not involved in the emulsion formation process. Thus, it can be speculated that the Pd/MS-PAP-20 catalyst will exhibit higher catalytic activity in ethyl acetate/H$_2$O biphasic systems.

3.2. Performance Evaluation of the Interfacial Active Catalyst in the Oil/Water Two-Phase Catalysis. Initially, a series of Pd-based heterogeneous catalysts were investigated on the hydrogenation of nitrobenzene in the toluene/H$_2$O biphasic system. The catalytic results show that the conversion of nitrobenzene is 55.1%, 72.5%, 75.6%, 88.3%, 96.9%, 87.9%, and 79.5% for Cat-0, Cat-5, Cat-10, Cat-15, Cat-20, Cat-25, and Cat-30, respectively. Among them, the Pd/MS-PAP-20 catalyst (Cat-20) exhibits the best catalytic activity for nitrobenzene hydrogenation. To further investigate the effect of solvent on the catalytic performance of the Pd/MS-PAP-20 catalyst, H$_2$O, ethyl acetate, ethyl acetate/H$_2$O, toluene/H$_2$O, and cyclohexane/H$_2$O were tested in the hydrogenation of nitrobenzene under identical reaction conditions. As shown in Figure 6b, the conversion of nitrobenzene is only 26.1% in the aqueous solution at 25 °C after 30 min of reaction, whereas the conversion of nitrobenzene is significantly increased to 99.5% in ethyl acetate/H$_2$O biphasic systems, which is similar to pure ethyl acetate. It is also observed that the catalyst also affords high catalytic activity in other oil/water biphasic systems (96.9% in toluene/H$_2$O and 91.5% in cyclohexane/H$_2$O) compared with the H$_2$O monophasic system. The enhancement of catalytic properties of the Pd/MS-PAP-20 catalyst in the oil/water biphasic system is predominantly attributed to the formation of countless microsized emulsion droplets, resulting in a larger oil/water contact area and lower mass transfer of the reaction partners as we previously reported.[37,38]

To explore the scope of the Pd/MS-PAP-20-catalyst-stabilized Pickering catalytic system for the hydrogenation of nitroarenes, a series of nitroarenes with structurally divergent functional groups and replacement positions are examined. The optimum reaction conditions for the hydrogenation of nitroarenes are given in Table 1. It can be seen that both nitrobenzene conversion and aniline selectivity are more than 99% in the presence of Pd/MS-PAP-20 catalyst within 30 min.

When the reaction is carried out using 5 wt % Pd/C as the catalyst, the conversion of nitrobenzene is very low (63.2%) even after 60 min. The superior catalytic performance of the Pd/MS-PAP-20 catalyst is probably because the formation of Pickering emulsions can significantly enhance the interfacial area in oil/water biphasic systems and decrease the mass transfer limitation of the substrate. The shape and size of the Pd/MS-PAP-20-stabilized emulsion are presented in Figure 5a,d. The catalyst can also quickly convert the nitroarenes with electron-donating groups (Table 1, entries 3−11) and electron-withdrawing groups (Table 1, entries 12−15) into the corresponding aniline derivatives, and the selectivity is above 99% within 60 min, except for 4-chloronitrobenzene. It should be pointed out that the hydrogenation of 4-chloronitrobenzene exists in the dechlorination phenomenon and the byproduct is mainly aniline. Hence, Pd/MS-PAP-20 is a universal and efficient interfacial catalyst for the selective hydrogenation of various nitroarenes in oil/water biphasic systems.

The stability and recyclability of the catalyst are a key factor for heterogeneous catalytic reactions. After each reaction, the product and the catalyst are, respectively, distributed into the ethyl acetate and water phase through centrifugation. The upper oil phase is withdrawn from the reaction system using a plastic straw, and fresh solvent and reactant are added into the aqueous phase containing the catalyst and reused in subsequent runs under identical reaction conditions. As shown in Figure 7, the Pd/MS-PAP-20 catalyst shows significantly high catalytic activity for the nitrobenzene hydrogenation, and the conversion remains >98% during the first five recycles, except that the conversion of nitrobenzene is reduced to 78.6% at the sixth run within 30 min. However, when the reaction time is slightly increased to 60 min after the sixth run, the nitrobenzene conversion reaches up to 96.2%. The content of Pd in the filtration is measured through inductively coupled plasma-optical emission spectroscopy (ICP-OES), which reveals that the leaching of Pd NPs from the support surface can be negligible. The recyclability result further demonstrates that the Pd NPs are well-encapsulated in the mesoporous channels and immobilized by the abundant amine groups.

4. CONCLUSIONS

In summary, we have successfully developed a facile strategy to synthesize interfacial active MS catalysts by one-pot cohydrolysis of PAPTMS and TMOS organosilanes. The hydrophilicity/hydrophobicity of the MS surface can be conveniently adjusted by altering the molar content of PAPTMS relative to the TMOS silica source precursor. Optical microscopy reveals that the Pd/MS-PAP-20 catalyst can be used as an emulsifier to create a stable water-in-oil-type Pickering emulsion in ethyl acetate/H$_2$O two-phase systems. Moreover, the prepared Pd/MS-PAP-20 catalyst-stabilized Pickering emulsion can efficiently reduce nitroarenes to target products in oil/water biphasic systems because of the countless microsized reactors and decreased mass-transport limitation. Therefore, our prepared interfacial active MS catalyst simplifies the separation and recovery of products and the catalyst, meanwhile providing new possibilities for various organic transformation reactions in biphasic systems. Further research relative to the present work is going on.

ASSOCIATED CONTENT

ⓢ Supporting Information

The Supporting Information is available free of charge on the ACS Publications website at DOI: 10.1021/acsomega.6b00209.

High-resolution transmission electron microscopy images of MS-PAP-20 microsphere, Pd NP size distribution of the Pd/MS and Pd/MS-PAP-20 catalysts, dispersion state of hydrophilic MS and relatively hydrophobic MS-PAP-20 in deionized water, and the results of N_2 adsorption–desorption of the as-prepared mesoporous materials (PDF)

AUTHOR INFORMATION

Corresponding Authors

*E-mail: fwzhang@sxu.edu.cn (F.Z.).
*E-mail: hqyang@sxu.edu.cn (H.Y.).
*E-mail: xmzhang@sxu.edu.cn. Phone: +86-351-7016082 (X.-M.Z.).

Notes

The authors declare no competing financial interest.

ACKNOWLEDGMENTS

REFERENCES

(1) Wu, T.; Wang, H.; Jing, B.; Liu, F.; Burns, P. C.; Na, C. Multi-Body Coalescence in Pickering Emulsions. *Nat. Commun.* **2015**, *6*, 5929.

(2) Flores, J. A.; Pavía-Sanders, A.; Chen, Y.; Pochan, D. J.; Wooley, K. L. Recyclable Hybrid Inorganic/Organic Magnetically Active Networks for the Sequestration of Crude Oil from Aqueous Environments. *Chem. Mater.* **2015**, *27*, 3775–3782.

(3) Chen, Z.; Zhao, C.; Ju, E.; Ji, H.; Ren, J.; Binks, B. P.; Qu, X. Design of Surface-Active Artificial Enzyme Particles to Stabilize Pickering Emulsion for High-Performance Biphasic Biocatalysis. *Adv. Mater.* **2016**, *28*, 1682–1688.

(4) Pera-Titus, M.; Leclercq, L.; Clacens, J.-M.; Campo, F. D.; Nardello-Rataj, V. Pickering Interfacial Catalysis for Biphasic Systems: From Emulsion Design to Green Reactions. *Angew. Chem., Int. Ed.* **2015**, *54*, 2006–2021.

(5) Huo, C.; Li, M.; Huang, X.; Yang, H.; Mann, S. Membrane Engineering of Colloidosome Microcompartments Using Partially Hydrophobic Mesoporous Silica Nanoparticles. *Langmuir* **2014**, *30*, 15047–15052.

(6) Wu, C.; Bai, S.; Ansorge-Schumacher, M. B.; Wang, D. Nanoparticle Cages for Enzyme Catalysis in Organic Media. *Adv. Mater.* **2011**, *23*, 5694–5699.

(7) Yang, Y.; Zhou, W.-J.; Liebens, A.; Clacens, J.-M.; Pera-Titus, M.; Wu, P. Amphiphilic Titanosilicates as Pickering Interfacial Catalysts for Liquid-Phase Oxidation Reactions. *J. Phys. Chem. C* **2015**, *119*, 25377–25384.

(8) Pickering, S. U. CXCVI.—Emulsions. *J. Chem. Soc., Trans.* **1907**, *91*, 2001–2021.

(9) Binks, B. P. Particles as Surfactants—Similarities and Differences. *Curr. Opin. Colloid Interface Sci.* **2002**, *7*, 21–41.

(10) Böker, A.; He, J.; Emrick, T.; Russell, T. P. Self-Assembly of Nanoparticles at Interfaces. *Soft Matter* **2007**, *3*, 1231–1248.

(11) Niu, Z.; He, J.; Russell, T. P.; Wang, Q. Synthesis of Nano/Microstructures at Fluid Interfaces. *Angew. Chem., Int. Ed.* **2010**, *49*, 10052–10066.

(12) Zhou, W.-J.; Fang, L.; Fan, Z.; Albela, B.; Bonneviot, L.; De Campo, F.; Pera-Titus, M.; Clacens, J.-M. Tunable Catalysts for Solvent-Free Biphasic Systems: Pickering Interfacial Catalysts over Amphiphilic Silica Nanoparticles. *J. Am. Chem. Soc.* **2014**, *136*, 4869–4872.

(13) Chevalier, Y.; Bolzinger, M.-A. Emulsions Stabilized with Solid Nanoparticles: Pickering Emulsions. *Colloids Surf., A* **2013**, *439*, 23–34.

(14) Liu, H.; Wang, C.; Gao, Q.; Liu, X.; Tong, Z. Magnetic Hydrogels with Supracolloidal Structures Prepared by Suspension Polymerization Stabilized by Fe_2O_3 Nanoparticles. *Acta Biomater.* **2010**, *6*, 275–281.

(15) Kylián, O.; Choukourov, A.; Biederman, H. Nanostructured Plasma Polymers. *Thin Solid Films* **2013**, *548*, 1–17.

(16) Kango, S.; Kalia, S.; Celli, A.; Njuguna, J.; Habibi, Y.; Kumar, R. Surface Modification of Inorganic Nanoparticles for Development of Organic-Inorganic Nanocomposites—A Review. *Prog. Polym. Sci.* **2013**, *38*, 1232–1261.

(17) Peng, J.; Liu, Q.; Xu, Z.; Masliyah, J. Novel Magnetic Demulsifier for Water Removal from Diluted Bitumen Emulsiion. *Energy Fuels* **2012**, *26*, 2705–2710.

(18) Kokal, S. L. Crude Oil Emulsions: A State-of-the-Art Review. *SPE Prod. Facil.* **2005**, *20*, 5–13.

(19) Stefaniu, C.; Chanana, M.; Wang, D.; Novikov, D. V.; Brezesinski, G.; Möhwald, H. Biocompatible Magnetite Nanoparticles Trapped at the Air/Water Interface. *ChemPhysChem* **2010**, *11*, 3585–3588.

(20) Ma, S.; Wang, Y.; Jiang, K.; Han, X. Decoratable Hybrid-Film-Patch Stabilized Pickering Emulsions and Their Catalytic Applications. *Nano Res.* **2015**, *8*, 2603–2610.

(21) Yu, C.; Fan, L.; Yang, J.; Shan, Y.; Qiu, J. Phase-Reversal Emulsion Catalysis with CNT-TiO_2 Nanohybrids for the Selective Oxidation of Benzyl Alcohol. *Chem.—Eur. J.* **2013**, *19*, 16192–16195.

(22) Teong, S. P.; Yi, G.; Zeng, H.; Zhang, Y. The Effects of Emulsion on Sugar Dehydration to 5-Hydroxymethylfurfural in a Biphasic System. *Green Chem.* **2015**, *17*, 3751–3755.

(23) Jiang, Y.; Liu, X.; Chen, Y.; Zhou, L.; He, Y.; Ma, L.; Gao, J. Pickering Emulsion Stabilized by Lipase-Containing Periodic Mesoporous Organosilica Particles: A Robust Biocatalyst System for Biodiesel Production. *Bioresour. Technol.* **2014**, *153*, 278–283.

(24) Crossley, S.; Faria, J.; Shen, M.; Resasco, D. E. Solid Nanoparticles that Catalyze Biofuel Upgrade Reactions at the Water/Oil Interface. *Science* **2010**, *327*, 68–72.

(25) Shi, D.; Faria, J.; Pham, T. N.; Resasco, D. E. Enhanced Activity and Selectivity of Fischer–Tropsch Synthesis Catalysts in Water/Oil Emulsions. *ACS Catal.* **2014**, *4*, 1944–1952.

(26) Faria, J.; Ruiz, M. P.; Resasco, D. E. Carbon Nanotube/Zeolite Hybrid Catalysts for Glucose Conversion in Water/Oil Emulsions. *ACS Catal.* **2015**, *5*, 4761–4771.

(27) Shi, D.; Faria, J. A.; Rownaghi, A. A.; Huhnke, R. L.; Resasco, D. E. Fischer–Tropsch Synthesis Catalyzed by Solid Nanoparticles at the Water/Oil Interface in an Emulsion System. *Energy Fuels* **2013**, *27*, 6118–6124.

(28) Qu, Y.; Huang, R.; Qi, W.; Su, R.; He, Z. Interfacial Polymerization of Dopamine in a Pickering Emulsion: Synthesis of Cross-Linkable Colloidosomes and Enzyme Immobilization at Oil/Water Interfaces. *ACS Appl. Mater. Interfaces* **2015**, *7*, 14954–14964.

(29) Fu, L.; Li, S.; Han, Z.; Liu, H.; Yang, H. Tuning the Wettability of Mesoporous Silica for Enhancing the Catalysis Efficiency of Aqueous Reactions. *Chem. Commun.* **2014**, *50*, 10045–10048.

(30) Zhang, F.; Yang, H. Multifunctional Mesoporous Silica-Supported Palladium Nanoparticles for Selective Phenol Hydrogenation in the Aqueous Phase. *Catal. Sci. Technol.* **2015**, *5*, 572–577.

(31) Tunlert, A.; Prasassarakich, P.; Poompradub, S. Antidegradation and Reinforcement Effects of Phenyltrimethoxysilane- or N-[3-(trimethoxysilyl)propyl]aniline-modified Silica Particles in Natural Rubber Composites. *Mater. Chem. Phys.* **2016**, *173*, 78–88.

(32) Mathew, A.; Parambadath, S.; Park, S. S.; Ha, C.-S. Hydrophobically Modified Spherical MCM-41 as Nanovalve System for Controlled Drug Delivery. *Microporous Mesoporous Mater.* **2014**, *200*, 124–131.

(33) Dai, C.-F.; Weng, C.-J.; Chien, C.-M.; Chen, Y.-L.; Yang, S.-Y.; Yeh, J.-M. Using Silane Coupling Agents to Prepare Raspberry-Shaped Polyaniline Hollow Microspheres with Tunable Nanoshell Thickness. *J. Colloid Interface Sci.* **2013**, *394*, 36−43.

(34) Kim, B.-J.; Kang, K.-S. Stopband Attenuation of Silica Spheres by Attaching Aniline and Polyaniline. *Synth. Met.* **2013**, *169*, 55−58.

(35) Wheelwright, W. V. K.; Ray, S.; Easteal, A. J. A Novel Low Solvent Method for Grafting Polyaniline to Silylated Silica. *Macromol. Symp.* **2010**, *298*, 51−56.

(36) Duan, L.; Fu, R.; Zhang, B.; Shi, W.; Chen, S.; Wan, Y. An Efficient Reusable Mesoporous Solid-Based Pd Catalyst for Selective C2 Arylation of Indoles in Water. *ACS Catal.* **2016**, *6*, 1062−1074.

(37) Chen, S.; Zhang, F.; Yang, M.; Li, X.; Liang, H.; Qiao, Y.; Liu, D.; Fan, W. A Simple Strategy towards the Preparation of a Highly Active Bifunctionalized Catalyst for the Deacetalization Reaction. *Appl. Catal., A* **2016**, *513*, 47−52.

(38) Liu, H.; Zhang, Z.; Yang, H.; Cheng, F.; Du, Z. Recycling Nanoparticle Catalysts without Separation Based on a Pickering Emulsion/Organic Biphasic System. *ChemSusChem* **2014**, *7*, 1888−1900.